

# The numerical analysis of the influence conductivity of clinker bricks and the size of their hollows on the distribution of the electromagnetic field

**Abstract.** The aim of this article is to present the analysis of the effects connected with the propagation of electromagnetic waves within an area containing non-ideal, non-homogenous and absorbing dielectric. The presented situation is one of the distribution of electromagnetic field generated by a wireless communication system operating within the standard frequency ( $f=2.4\text{GHz}$ ). The analysis included single and double layered walls used in housing construction, built from hollow clay bricks with different amounts of holes. The results were then compared with identical versions of walls built from solid brick. The influence of the size of holes, the contained clay mass percentage and its conductivity on the distribution of electromagnetic field was discussed.

**Streszczenie.** Celem publikacji jest przedstawienie analizy zjawisk związanych z propagacją fal elektromagnetycznych w obszarze zawierającym ścianę złożoną z nieidealnego, niejednorodnego, absorbującego dielektryka. Zaprezentowany został rozkład pola elektromagnetycznego generowanego przez system komunikacji bezprzewodowej pracujący przy standardowej częstotliwości ( $f=2,4\text{GHz}$ ). Analiza dotyczyła stosowanych w budownictwie jednorodzinnych ścian jedno oraz dwuwarstwowych wykonanych z cegieł klinkierowych z różną ilością drążów. Wyniki porównano z analogicznymi wariantami ścian złożonych z pełnych cegieł. Omówiono wpływ rozmiaru drążów, procentowej zawartości masy ceramicznej oraz jej przewodności na rozkład pola elektromagnetycznego. (Numeryczna analiza wpływu przewodności cegieł klinkierowych i rozmiaru ich drążów na rozkład pola elektromagnetycznego).

**Keywords:** electromagnetic waves propagation, finite difference time domain method (FDTD), wireless communication, building materials.  
**Słowa kluczowe:** propagacja fal elektromagnetycznych, metoda różnic skończonych w dziedzinie czasu (FDTD), komunikacja bezprzewodowa, materiały budowlane.

## Introduction

Modern building technology is based mainly on clay materials and layers of walls depending on the used materials and the final function of the construction. Single-family buildings contain single and multi-layered walls consisting mainly of various kind of bricks, silicate blocks or autoclaved aerated concrete. The location of wireless communication systems (Wi-Fi) inside this type of a building requires an analysis of the changes which occur during the propagation of electromagnetic wave. The above mentioned notion has been a subject of many scientific research to date [1-7]. However, the majority of the authors focuses on the analysis of homogenous building materials i.e. concrete slabs or solid brick. This type of scenario has a predictable distribution of the EM field and the solution can be achieved through the use of analytical methods [5, 8]. It needs to be stressed that the distribution of the field inside rooms is influenced not only by damping of the wave, but also multiple reflections caused by the geometry of the area and the complex structure of the building material.

This article presents the analysis of the distribution of EM field in an area containing a single or double-layered wall made of various kinds of bricks. Due to the variability of the electrical properties of a brick claimed by different authors, like its electrical permittivity ( $\epsilon_r=3.7\div 19$  [9],  $\epsilon_r=4.62\div 4.11$  [5], or conductivity ( $\sigma=0.00278\div 0.244\text{ S/m}$ ) [4-6] the maximum values of the  $E_z$  component were analysed in the function of conductivity value. Additionally, the value of the EM field was analysed in the function of the percentage of clay mass in the brick.

The assessment of the field created as the result of EM wave propagation through a wall made of various types of bricks will allow us to understand the processes which take place in environments with a non-homogenous dielectric.

## Analysed models

In the macroscopic approach, reinforced concrete and hollow bricks are classified as complex building structures. In such circumstances the assessment of the distribution of the field may only be performed by usage of numerical analysis. In this article, the presented analysis is of three

commonly used walls made of three types of building material:

- 1) solid brick,
- 2) hollow clay brick with 18 vertical holes (marked as B18) (Fig. 1a),
- 3) hollow clay brick with 30 vertical holes (B30) (Fig. 1b).

The analysed problem, in an electrical sense, is limited to the analysis of the porous elements because:

- the EM wave propagates through a multi-layered structure comprised of air and a non-ideal dielectric i.e. a diffusing clay mass,
- there is a periodic arrangement of materials,
- the dimensions of the brick and holes (with the analysed frequency of  $f=2.4\text{GHz}$ ) are comparable to the length of the EM wave propagating in air  $\lambda_a=0.125\text{ m}$  (Fig. 1).

Fig. 1 is a representation of the dimensions of bricks and their electrical reproduction, where  $\lambda_b=0.0593\text{ m}$  is the length of the wave in a clay material.

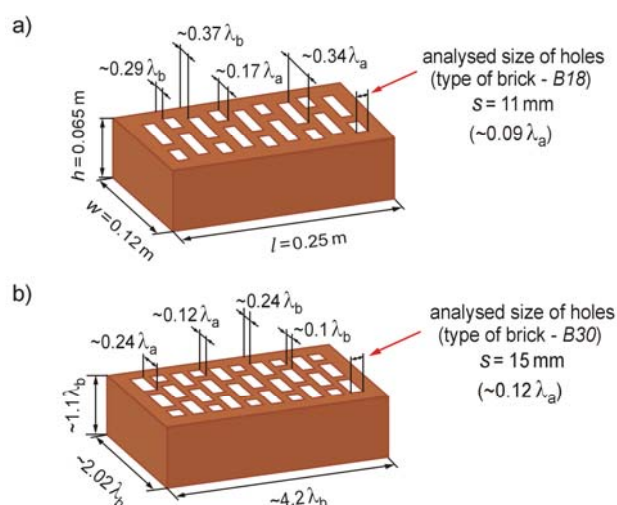


Fig.1. Electrical and geometrical sizes of two types of analysed brick: a) B18 and b) B30

Additionally the variability of the width of the holes was analysed ( $s$ ) along the length of the brick ( $l$ ) assuming that  $s \in \{0, 0.005, 0.007, 0.011, 0.013, 0.015, 0.017, 0.019\}$  m. The size of the hole influences the percentage share of the loss dielectric (clay mass) in the brick ( $v$ ) (Table 1). Red colour signifies the values of the typical hole sizes in two types of hollow clay bricks. Bold type was used to signify the two closest  $v$  values in various sizes of holes.

Table 1. The percentage of the clay inside the analysed bricks dependent on the size of holes

Geometric size of holes ( $s$ ) inside the brick [m], changed along axis $Ox$ (Figs. 1, 2)	Relative volume of the clay in the brick ( $v$ ) [%]	
	Brick (B18)	Brick (B30)
0.005	90.40	87.50
0.007	86.56	<b>82.50</b>
0.009	<b>82.72</b>	77.50
0.011	<b>78.88</b>	72.50
0.013	75.04	<b>67.50</b>
0.015	71.20	<b>62.50</b>
0.017	<b>67.36</b>	57.50
0.019	63.52	52.50

The analysis was of single (0.12 m) and double-layered walls (0.24 m) consisting of solid bricks, B18 or B30 (Fig. 2a-d). The dimensions and numerical conditions of the analysed area in one of the four variants of walls (i.e. double-layered wall made of B18 bricks) has been presented in Fig. 2e.

The origin of the field was a sinusoidally oscillating plane wave with a frequency of  $f=2.4$  GHz. The EM field is excited in a region far away of the wall. The absorption of the incident and reflected waves are obtained using PML boundary conditions (*perfectly matched layer*) [10]. These were entered in the outside areas, perpendicular to the equiphase surface.

The main goal of this analysis was to determine the value of the field in the area behind the wall. It was assumed that the crosswise dimensions of the wall are significantly larger than the dimensions of the brick and the length of the wave. Incidents at the edges of the wall were ignored and periodic boundary conditions were assumed. The length of the wall was reduced to three bricks ( $l \approx 3$ ), whereas in the edges perpendicular to the  $Ox$  axis, Bloch's periodic boundary conditions were assumed [11].

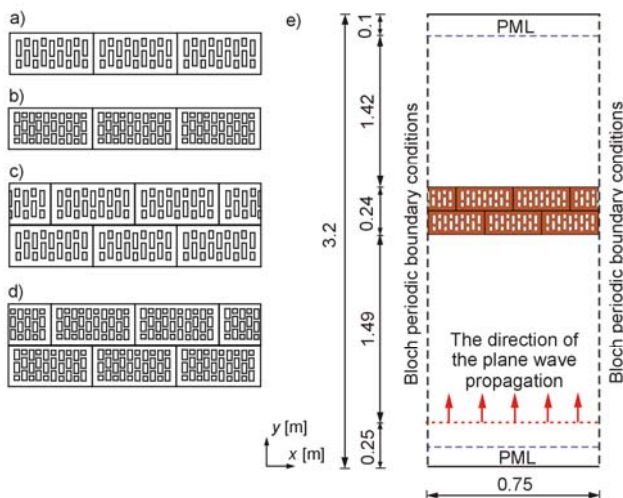


Fig.2. The four kinds of analysed wall (a-d) and the geometry with numerical conditions for all models of wall (e)

To analyse the researched variants, a relative electrical permittivity of  $\epsilon_r=4.44$  was determined [4-5], whereas the conductivity was modified within the range  $\sigma=0 \div 0.2$  S/m.

### Numerical model

To determine the distribution of the electromagnetic field, the finite difference time domain method (FDTD) was used [10]. This method is useful in the numerical analysis of high frequency time dependent electromagnetic fields.

The FDTD method is based on the direct numerical integration of the Maxwell curl equations in time and space [8, 10]. These equations are directly integrated in time and space domains.

$$(1) \quad \nabla \times \vec{H} = \sigma \vec{E} + \epsilon \frac{\partial \vec{E}}{\partial t}$$

$$(2) \quad \nabla \times \vec{E} = -\mu \frac{\partial \vec{H}}{\partial t}$$

The examined area is divided into elementary cubic Yee cells. For each cell three components are then assigned for both field  $\vec{E}$  and  $\vec{H}$  respectively, which are calculated in different points of space. The displacement of discrete time values by  $\Delta t/2$  that appears in the calculations is used to determine the electric field with respect to the values, where the magnetic field is calculated.

The stability of the time marching explicit scheme requires satisfying the Courant-Friedrichs-Lewy (CFL) condition [7, 10], which determines the relationship between time step in the leap-frog scheme of FDTD method and the maximum size of Yee cell [10].

The analyzed area was composed of Yee cells (0.0016667 m). Due to this, the length of the wave in the air ( $\lambda_a$ ) corresponded to 75 Yee cells,  $\lambda_b$  (30 Yee cells),  $s=0.011$  m (7 Yee cells),  $s=0.015$  m (9 Yee cells). The total number of Yee cells for each model amounted to 864000. The analysis of the electromagnetic field distribution was carried out with libraries delivered within the Meep package [11].

### Simulation results

Figure 3 shows the distribution of  $E_z$  component inside the analysed area. The results of calculation are shown in the  $XY$  plane at the time when the steady state of the EM field distribution had been achieved.

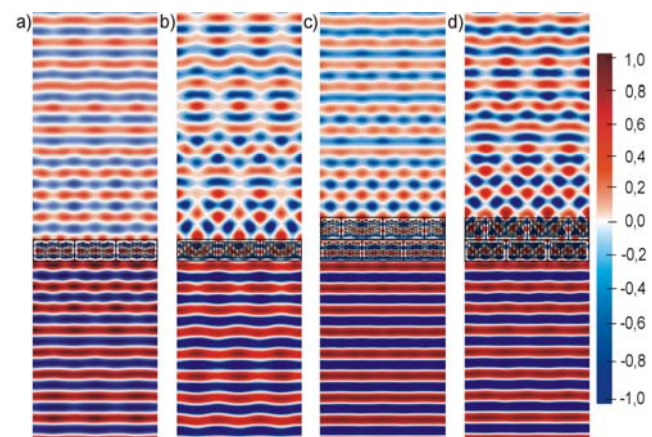


Fig.3. A snapshot of the 2D distribution of relative value of  $E_z$  component inside analysed area with the wall made of bricks: a) B18 (one layer), b) B30 (one layer), c) B18 (two layers) and d) B30 (two layers)

A local change of the EM wave's speed in passing through different areas of the brick leads to the creation of temporary images of the field. This proves the occurrence

of interference. The discussed effect is especially visible while assessing the effects occurring behind a wall made of *B30* bricks. The field behind the wall has higher values both minimum and maximum.

The difference in the percentage of clay mass in both types of brick (*B18* –  $s=0.011$  m and *B30* –  $s=0.015$  m) is 16.38%. As shown in Fig. 3 (a, c) higher  $v$  causes lower distortion of the wave front. At the same time, due to damping, it influences negatively the ability to acquire higher field values. An example analysis of single-layered walls – relative maximum values of the  $E_z$  component for the model made of *B18* bricks are lower by around 12% in comparison to *B30*.

Figures 4-7 show the relative maximum values of the  $E_z$  component and their dependencies on the size of holes ( $s$ ) and variability of conductivity.

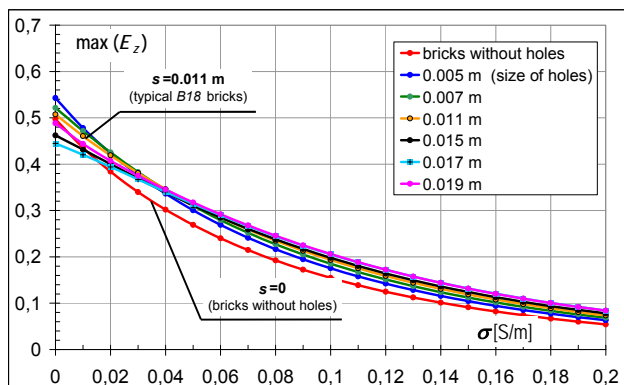


Fig.4. The relative maximum values of  $E_z$  component behind the wall made of *B18* bricks (one layer)

Analysis has shown that the decrease of  $v$  for the actual dimensions of the holes i.e.  $s \in \{0.007, 0.011, 0.015\}$  m} together with an increase in conductivity causes an increase of the maximum values of the  $E_z$  component (ex. for  $\sigma=0.1$  S/m – an increase by 20%;  $\sigma=0.2$  S/m – an increase by 50%).

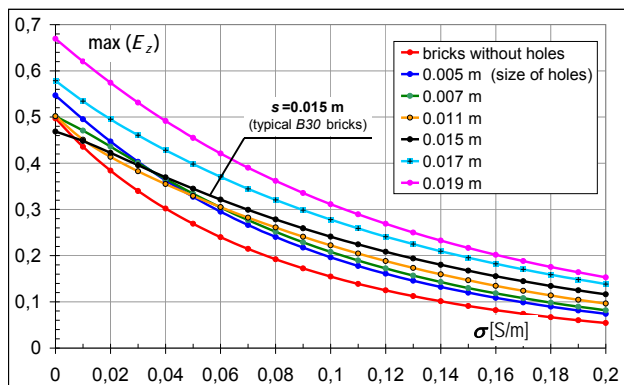


Fig.5. The relative maximum values of  $E_z$  component behind the wall made of *B30* bricks (one layer)

In Fig. 5 for characteristics with the size of holes  $s \in \{0.017, 0.019\}$  m}, an increase in the relative maximum values of the  $E_z$  component can be seen. Such tendency is a result of the multiple reflections occurring within the material containing almost 50% relative volume of the clay in the brick ( $s=0.017$  -  $v=57.5\%$  and  $s=0.019$  m -  $v=52.5\%$ ). Taking into account the norms such variants of brick are not acceptable in mass production and therefore such characteristics should not be analysed in detail.

From the characteristics in Figs. 4, 5 it may be claimed that the differences between the graphs representing the

dependence of conductivity on the size of the holes in brick *B30* are on average twice as high than in the *B18* model. For example, for  $\sigma=0.1$  S/m and type *B18* brick the value of the observed component for  $s=0.015$  m is higher by around 5% than for  $s=0.011$  m, whereas in the other brick type (*B30*) this difference is around 10%.

In Fig. 6 (for a double-layered wall) the characteristics presented, point to a decrease of the maximum value of the  $E_z$  component, where for example for  $\sigma=0.09$  S/m the presented values are consistent with those acquired for a single-layered wall for  $\sigma=0.19$  S/m. At the same time, for  $\sigma=0.05$  S/m the maximum values of the  $E_z$  component are the same in both the absence of holes and for  $s=0.005 \div 0.011$  m.

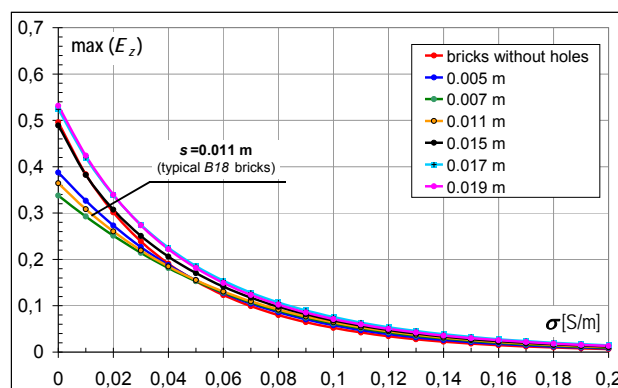


Fig.6. The relative maximum values of  $E_z$  component behind the wall made of *B18* bricks (two layers)

In Fig. 7 for a double-layered wall (*B30*) a more rapid decrease of the maximum value of the  $E_z$  component can be observed, than in the case of a single-layered wall (Fig. 5). In this variant, the hole dimension being irrelevant, smaller differences between the characteristics are visible than in the distribution of maximum relative values of the  $E_z$  component for a single-layered wall.

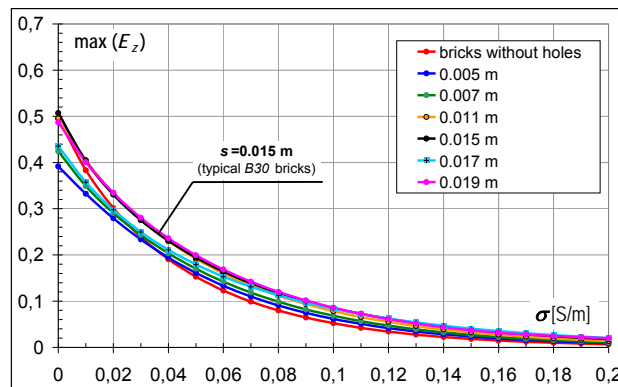


Fig.7. The relative maximum values of  $E_z$  component behind the wall made of *B30* bricks (two layers)

In Figs. 8-11 the comparison of the increase of the maximum relative value of the  $E_z$  component is presented in dependence to the percentage of clay mass in the analysed wall models in the range of the most often used values of conductivity.

Basing on the presented graphs, it may be claimed that the comparable  $v$  value (Table 1) does not influence achieving of the predicted maximum values of the  $E_z$  component. The reason for this are the multiple reflections and interference at the air-clay border.

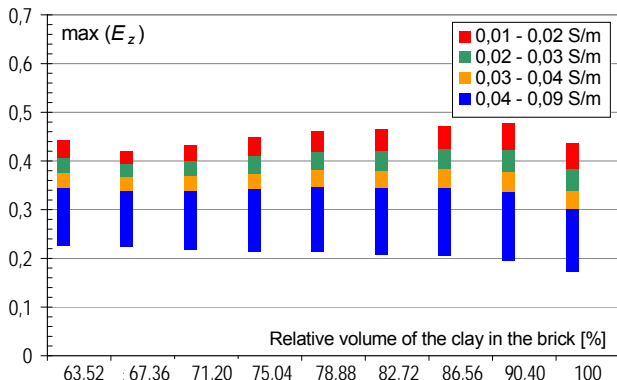


Fig.8. The dependence between relative maximum values of  $E_z$  component and the relative volume of the clay in the B18 brick for one layer wall

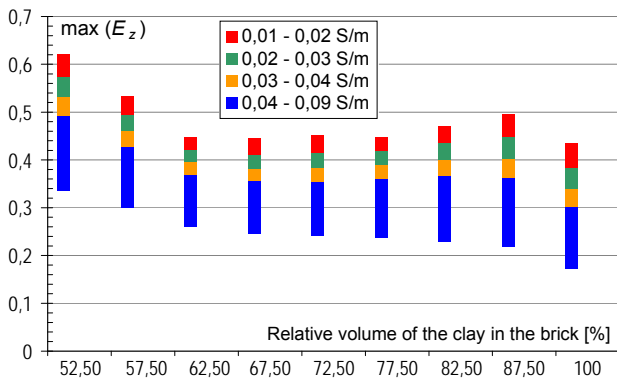


Fig.9. The dependence between relative maximum values of  $E_z$  component and the relative volume of the clay in the B30 brick (one layer wall)

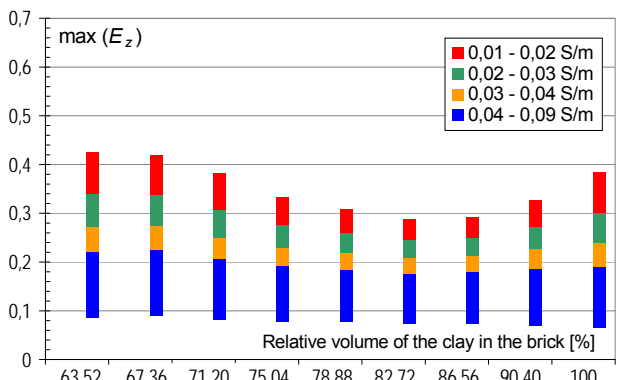


Fig.10. The dependence between relative maximum values of  $E_z$  component and  $v$  (two layers wall made of B18 bricks)

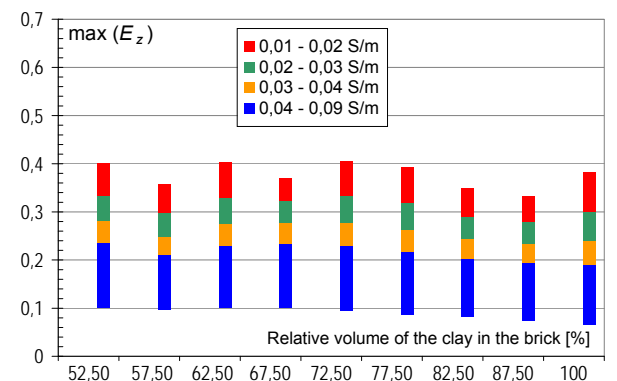


Fig.11. The dependence between relative maximum values of  $E_z$  component and  $v$  for B30 bricks (two layers)

## Conclusions

The propagation of EM wave in the area of brick is a complex process. The porous structure of the brick in an electromagnetic sense influences the occurrence of multiple reflections at the air-brick border. The number and size of the holes in the brick results in temporary changes of field image in the area close behind the wall. A local shift in the speed of the wave while passing through various parts of the brick is depicted in the distribution of the field and occurrence of interference. The differences in field value is greater in the case of B30 brick. A higher percentage of clay material in the wall causes smaller distortion of the wave front in the area behind the wall. When discussing the wall, in which the damping is insignificant ( $\sigma < 0.01$  S/m) or equals zero, interference effects play a much greater role. This may explain the non-monotonous course of characteristics and visible minimal values in some range of hole sizes.

## REFERENCES

- [1] Liu Ping, Chen Gui, Long Yun-liang, Effects of reinforced concrete walls on transmission of EM wave in WLAN, *Proceedings of the ICMMT 2008, International Conference on Microwave and Millimeter Wave Technology*, Vol. 2 (2008), 519-522
- [2] Peña D., Feick R., Hristov H.D., Grote W., Measurement and modeling of propagation losses in brick and concrete walls for the 900 MHz band, *IEEE Transactions on Antennas and Propagation*, 51 (2003), No. 1, 31-39
- [3] Yang M., Stavrou S., Rigorous coupled-wave analysis of radio wave propagation through periodic building structures, *IEEE Antennas and Wireless Propagation Letters*, Vol. 3 (2004), 204-207
- [4] Tan S.Y., Tan Y., Tan H.S., Multipath delay measurements and modeling for interfloor wireless communications, *IEEE Transactions on Vehicular Technology*, 49 (2000), No. 4, 1334-1341
- [5] Landron O., Feuerstein M.J., Rappaport T.S., A comparison of theoretical and empirical reflection coefficients for typical exterior wall surfaces in a mobile radio environment, *IEEE Transactions on Antennas and Propagation*, Vol. 44 (1996), No. 3, 341-351
- [6] Pinhasi Y., Yahalom A., Petnev S., Propagation of ultra wide-band signals in lossy dispersive media, *IEEE International Conference on Microwaves, Communications, Antennas and Electronic Systems, COMCAS* (2008), 1-10
- [7] Choroszucho A., Butryto B., Inhomogeneities and dumping of high frequency electromagnetic field in the space close to porous wall, *Przegląd Elektrotechniczny (Electrical Review)*, R. 88 (2012), nr 5a, 263-266
- [8] Morawski T., Gwarek T., Pola i fale elektromagnetyczne, WNT, Warszawa (1998)
- [9] Shah M.A., Hasted J.B., Moore L., Microwave absorption by water in building materials: aerated concrete, *British Journal of Applied Physics*, Vol. 16 (1965), No. 11, 1747-1754
- [10] Taflove A., Hagness S.C., Computational electrodynamics, The Finite-Difference Time-Domain Method. Boston, Artech House, (2005)
- [11] Oskooi A.F., Roundyb D., Ibanescua M., Bermelc P., Joannopoulousa J.D., Johnson S.G., MEEP: A flexible free-software package for electromagnetic simulations by the FDTD method, *Computer Physics Communications*, Vol. 181 (2010), 687-702

## Authors:

mgr inż. Agnieszka Choroszucho,  
E-mail: [a.choroszucho@pb.edu.pl](mailto:a.choroszucho@pb.edu.pl)

dr inż. Bogusław Butryto,  
E-mail: [b.butryto@pb.edu.pl](mailto:b.butryto@pb.edu.pl)

Politechnika Białostocka, Wydział Elektryczny, Katedra Elektrotechniki Teoretycznej i Metrologii, ul. Wiejska 45D, 15-351 Białystok.